

Matrix compare analysis discriminates subtle structural differences in a family of novel antiproliferative agents, diaryl-3-hydroxy-2,3,3a,10a-tetrahydrobenzo[*b*]-cyclopenta[*e*]azepine-4,10(1*H*,5*H*)-diones

Conrad Kunick,^{a,*} Carola Bleeker,^b Christian Prühs,^a Frank Totzke,^c Christoph Schächtele,^c Michael H. G. Kubbutat^c and Andreas Link^d

^aTechnische Universität Braunschweig, Institut für Pharmazeutische Chemie, Beethovenstrasse 55, D-38106 Braunschweig, Germany

^bUniversität Hamburg, Institut für Pharmazie, Bundesstrasse 45, D-20146 Hamburg, Germany

^cProQinase GmbH, Breisacher Strasse 117, 79106 Freiburg, Germany

^dErnst-Moritz-Arndt-Universität Greifswald, Institut für Pharmazie, Friedrich-Ludwig-Jahn-Strasse 17, 17487 Greifswald, Germany

Received 7 December 2005; revised 13 January 2006; accepted 13 January 2006

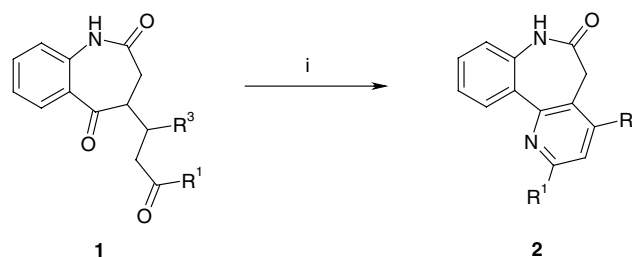
Available online 7 February 2006

Abstract—A diastereoselective synthesis of diaryl-3-hydroxy-2,3,3a,10a-tetrahydrobenzo[*b*]cyclopenta[*e*]azepine-4,10(1*H*,5*H*)-diones is described employing a tandem Michael-aldol addition as key step. The novel compounds exhibit antiproliferative activity in a panel of in vitro cultivated cancer cell lines. The bioinformatic tool COMPARE was able to discriminate between two closely related subgroups of the title compounds, namely 1,3- and 2,3-disubstituted derivatives.

© 2006 Elsevier Ltd. All rights reserved.

The darpones **2** are a class of compounds displaying in vitro and in vivo antiproliferative activity against tumor cells. The biochemical mechanism underlying the growth inhibitory effects of darpones is still unknown.^{1–4} For the general synthesis of darpones, the oxidative cyclization of the 1,5-diones **1** is a key step (Scheme 1). The intermediates **1** are prepared by Michael addition reactions of the 1*H*-[1]benzazepine-2,5(3*H*,4*H*)-dione **3** and 1,3-diarylpropenones **4** in the presence of 0.1 equivalents of potassium hydroxide.¹ Serendipitously, we found that upon employing higher concentrations of the basic catalyst, a tandem Michael-aldol addition leads diastereoselectively from the mentioned starting materials to a new compound class, namely 1,3-diaryl-3-hydroxy-2,3,3a,10a-tetrahydrobenzo[*b*]cyclopenta[*e*]azepine-4,10(1*H*,5*H*)-diones **5** (Scheme 2).

Because **5** bear a weak structural resemblance to the darpones **2**, the former were tested in the In Vitro Cell Line



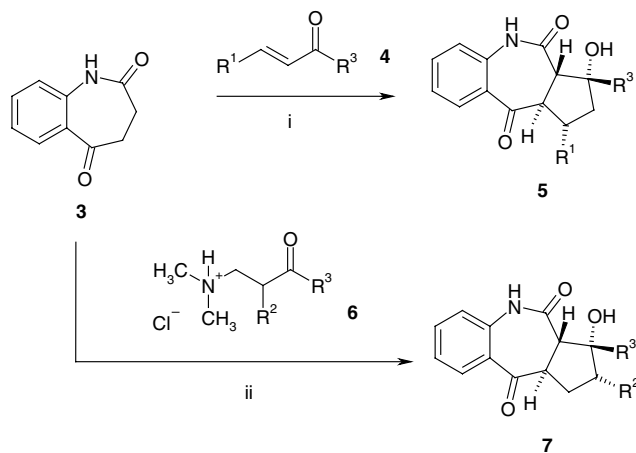
Scheme 1. Synthesis of darpones **2**. Reagents and conditions: (i) NH_4OAc , $\text{NH}_4\text{Fe}(\text{SO}_4)_2$, AcOH , N_2 , reflux.

Screening Project (IVCLSP) of the American National Cancer Institute. Although the overall in vitro antiproliferative activity of **5a–g** was only modest with averaged growth inhibition values (mean graph midpoint values; MG MID) between 10 and 100 μM , distinct cancer cell lines were inhibited selectively, for example, the NSCL cancer cell line NCI-H460 (Table 1).

The reaction leading to **5** furnishes the depicted racemic (1*SR*,3*RS*,3a*SR*,10a*RS*) diastereomers. In the crude reaction mixtures, less than 10% of side diastereomers

Keywords: Compare analysis; Tandem Michael-aldol cyclization; Anticancer agents.

* Corresponding author. Fax: +49 531 3912799; e-mail: c.kunick@tu-bs.de



Scheme 2. Synthesis of diaryl-3-hydroxy-2,3,3a,10a-tetrahydrobenzo[*b*]-cyclopenta[*e*]azepine-4,10(1*H*,5*H*)-diones **5** and **7**. Reagents and conditions: (i) 1 equiv KOH, EtOH, rt; (ii) 2 equiv KOH, EtOH, rt.

were detected by NMR spectroscopy. These side products and traces of open chain precursors **1** were easily removed during the workup procedure which consisted of collecting the precipitate from the reaction mixture and crystallization from ethanol.

In order to structurally modify the parent motif **5**, it was intended to shift the 1-aryl substituent to the 2-position. For the synthesis of the so-designed 2,3-diaryl-3-hydroxy-2,3,3a,10a-tetrahydrobenzo[*b*]cyclopenta[*e*]azepine-4,10(1*H*,5*H*)-diones **7** by an analogous procedure, it would have been necessary to replace the chalcones **4** by 1,2-diarylpropenones. Since it is well known that the latter are relatively unstable due to formation of Diels–Alder dimers,⁵ the Mannich bases **6**^{6–8} were employed in the cyclization reactions as precursors for the corresponding 1,2-diarylpropenones. Again, upon treatment with potassium hydroxide in ethanol the products of tandem Michael–aldol cyclizations were formed diastereoselectively, albeit in poor to moderate yields (15–49%) (Table 1, entries **7a–g**). Again, side diastereomers were detected in the crude reaction mixtures only in a low extent (<10%). Both for compound series **5** and **7** the relative stereochemistry was determined by assignment of the aliphatic proton signals by COSY experiments and subsequent evaluation of NOESY spectra as exemplified for compound **7a** (Fig. 1).

In the IVCLSP, the 2,3-diaryl analogs **7** revealed an enhanced average antiproliferative potential compared to the 1,3-diaryl structures. Furthermore, a characteristic selectivity pattern with regard to the antiproliferative activity on specific cell lines was observed which appeared to be distinct of that found for the 1,3-diaryl analogs **5**. For example, the NSCL cancer cell line HOP-62, which was scarcely affected by members of the 1,3-diaryl series **5**, was inhibited by the 1,2-diaryl analogs **7** in low micromolar concentrations.

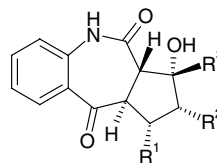
For a further rational development of the novel compound classes **5** and **7** as anticancer agents it is of high relevance to detect the biological targets underlying their antiproliferative activity. From structural similarity of **5**

or **7** to established anticancer agents such a mechanism is not obvious. However, the selectivity pattern of a compound displayed in the IVCLSP can be used to generate a hypothesis on the nature of the growth inhibition mechanism.

In the IVCLSP, the antiproliferative activities of test compounds are determined in vitro on distinct cancer cell lines from nine different tumor entities, representing leukemia, melanoma and cancers of the lung, colon, brain, ovary, breast, prostate, and kidney. For this purpose, the cancer cells are incubated with five concentrations between 10^{-8} and 10^{-4} M of the test compound for two days. A sulforhodamine B assay is employed to determine the surviving cells. GI_{50} values (GI_{50} = concentration to inhibit cell growth by 50%) are calculated for the single cell lines. An averaged GI_{50} value over all the cell lines in the screen is calculated defining the average antiproliferative activity of a test compound. This averaged parameter is designated meangraph midpoint (MG-MID).^{9,10}

The selectivity pattern of a compound displayed in the IVCLSP can be exploited for the generation of hypotheses regarding the mechanism of action of an antiproliferative compound. The basis for such a study is a COMPARE analysis which pairwise compares the selectivity patterns of two given compounds within the cell line panel of the IVCLSP. As a result of the COMPARE analysis a Pearson correlation coefficient (PCC, values between -1 and $+1$) is calculated. A high PCC suggests that two agents share a similar antiproliferative mechanism.^{9,11–13} To check whether the compound classes **5** and **7** display typical selectivity patterns and thus exhibit characteristic antiproliferative mechanisms, a matrix COMPARE analysis was performed in which all compounds listed in Table 1 were compared pairwise. From the results of the matrix COMPARE analysis given in Table 2 the high discriminatory capability of the tool becomes obvious: with just one single exception (correlation of **5b** and **7g**) significant ($p < 0.01$) correlations could not be detected when members of the two subgroups were compared (refer to values within the rectangle marked in Table 2). In contrast, within a subgroup a high pattern consistency was found: 13 out of 21 possible correlations were found significant within the subgroup **5**, and all 28 correlations in subgroup **7** were considered significant. These findings suggest that both compound classes **5** and **7** constitute groups of antiproliferative agents with different but characteristic mechanisms of action. In this context, it has to be stressed that the levels of significance (p values) are not indicating the potential biological meaning of a correlation but, rather, they are a measure of purely mathematical significance based on the relative variance of the two data sets being correlated.

COMPARE analyses with members of the **5** and **7** series in the NCI database of standard agents revealed that 4-nitro-estrone-4-methylether (NSC321803) and bleomycin (NSC 125066) were frequently ranked in the top positions of standard agents correlated to **7** (data not shown). However, since the two standard agents are not sharing an obvious common mechanism this observation is not helpful in the search for the biological targets of **7**.

Table 1. Structural, chemical, and physical data of diaryl-3-hydroxy-2,3,3a,10a-tetrahydrobenzo[*b*]cyclopenta[*e*]azepine-4,10(1*H*,5*H*)-diones **5** and **7**

Compound	R ¹	R ²	R ³	Yield (%)	mp (°C)	Log ₁₀ GI ₅₀ (M) HOP-62 ^b	Log ₁₀ GI ₅₀ (M) NCI-H460 ^c	Log ₁₀ GI ₅₀ (M) MG-MID ^d	Correlation with epidermal growth factor receptor (MT1093) ^{e,f}	Correlation with AXL (receptor tyrosine kinase) (MT994) ^{e,f}
5a	4-MeO-Ph	H	Ph	59	230–235	>−4.0	−5.1	−4.1	0.035 (53)	0.148 (53)
5b	4-Cl-Ph	H	Ph	39	238–239	>−4.0	−5.0	−4.1	0.095 (54)	0.195 (54)
5c	3-Cl-Ph	H	Ph	34	229–230	>−4.0	−5.2	−4.1	−0.170 (55)	−0.157 (55)
5d^a	Ph	H	3-Cl-Ph	39	224–225	>−4.0	−5.7	−4.5	−0.106 (59)	−0.130 (59)
5e^a	Ph	H	2-Naphthyl	42	238–239	>−4.0	−6.7	−4.8	−0.047 (59)	0.022 (59)
5f	Ph	H	1,3-Benzodioxol-5-yl	42	254 (dec)	−4.1	−5.6	−4.3	−0.185 (55)	−0.077 (55)
5g	4-MeO-Ph	H	3-Cl-Ph	60	236	>−4.0	−5.0	−4.2	−0.083 (49)	−0.108 (49)
7a	H	Ph	Ph	44	247–258 (dec)	−5.4	−5.4	−4.9	0.441 (59)	0.528 (49)
7b^a	H	4-Me-Ph	Ph	49	261–262 (dec)	−5.6	−5.1	−5.3	0.491 (59)	0.439 (59)
7c^a	H	4-MeO-Ph	Ph	29	261–263 (dec)	−5.6	−4.9	−4.9	0.480 (59)	0.505 (59)
7d^a	H	4-Cl-Ph	Ph	53	271–276 (dec)	−5.6	−5.4	−5.3	0.417 (59)	0.423 (59)
7e^a	H	3-Cl-Ph	Ph	33	244–247 (dec)	−5.1	−4.6	−4.7	0.368 (59)	0.376 (59)
7f^a	H	Ph	4-Me-Ph	15	286 (dec)	−5.4	−4.7	−4.8	0.493 (59)	0.536 (59)
7g^a	H	4-Me-Ph	4-Me-Ph	29	258–262 (dec)	−5.2	−5.4	−5.2	0.211 (59)	0.28 (59)
7h^a	H	4-Cl-Ph	4-Me-Ph	32	270–272 (dec)	−5.3	−5.7	−5.4	0.325 (59)	0.358 (59)

Antiproliferative activity of **5** and **7** in the In Vitro Cell Line Screening Project (IVCLSP) of the National Cancer Institute and correlation with selected molecular targets (MT) determined in the cell lines of the IVCLSP. Numbers in brackets correspond to the cell lines that were used for calculation.

^a Average of 2 experiments.

^b Non-small cell lung cancer cell line.

^c Non-small cell lung cancer cell line.

^d MG-MID, meangraph midpoint, mean value for all tested cancer cell lines. If the indicated effect was not attainable for distinct cell lines within the used concentration interval, the highest tested concentration (=100 μM) was used for the calculation.

^e The correlation (Pearson correlation coefficient, PCC) with RNA levels (log values) of the distinct target is given. Numbers in brackets correspond to the number of cell lines that were used for calculation.

^f The data given in bold italics are considered significant ($p < 0.01$). The distinct p values were calculated from the PCCs and the number of cell lines by StaTable vers.1.0.2 (Cytel Software, Cambridge, MA 02139, USA).

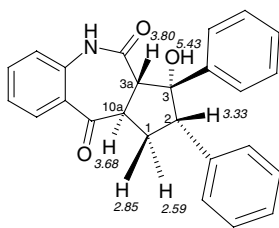


Figure 1. NOESY-assignment of the aliphatic and OH protons in compound **7a**. The signal of the HO proton in position 3 (5.43 ppm) displays cross-relations with the signals at 3.68 and 2.59 ppm, showing that these protons are located on one side of the cyclopentane plane. On the other side of the plane are located H-3a (3.80 ppm) and H-2 (3.33 ppm), as is demonstrated by a NOE. The stereochemical assumption depicted in Fig 1 is further supported by the observation of NOEs between the signals at 2.85 and 3.33 ppm on the one hand and between H-3a and signals caused by hydrogen nuclei of the phenyl substituent at C-3 on the other hand.

The NCI's database of molecular targets (MTs) contains expression levels of proven or putative biological targets determined in the cancer cell lines of the IVCLSP. A COMPARE analysis in the MTs database with the IVCLSP selectivity pattern of a test compound as seed might contribute hints to its mechanism of action, although it must be kept in mind that in this case two different patterns are compared: a pattern of endpoint (GI₅₀) determinations after two days of compound exposure and a pattern of target expression in steadily growing cells. The COMPARE with **5** and **7** in the molecular targets database revealed distinct entries that were frequently found in lists of MTs ranked by PCCs with compounds **7**; among others the positively correlated targets MT994 (AXL receptor tyrosine kinase),¹⁴ and MT1093 (epidermal growth factor receptor, EGFR),¹⁵ although the correlation coefficients were not high in absolute terms (for PCC values refer to Table 1). The only compound that is not exhibiting a significant correlation with any of these targets is derivative **7g**, which therefore has to be regarded as relatively untypical for the compound class. Of note, both molecular targets are tyrosine kinases that have been related to cancer, and of these the EGF receptor kinase is one of the main target molecules of kinase inhibitors that are currently clinically evaluated as antitumor drugs.¹⁶ In contrast, neither the AXL receptor tyrosine kinase nor the EGFR kinase was significantly correlated with a compound from series **5**. In order to gain information whether the antiproliferative activity of the novel structures is based on a direct inhibition of phosphorylating enzymes, representatives **5c** and **7a** from both series were tested in a commercially available screening system on 16 cancer-related kinases (Aurora-A, CDK4/CycD1, CDK2/CycE, EGFR, Erb-b2, PDGFR-beta, PLK1, AKT1, IGF1-R, VEGF-R1, VEGF-R2, VEGF-R3, TIE2, EPHB4, FAK, and SRC). In this preliminary assay, the compounds were tested in 10 μM concentrations in the presence of 0.1 μM ATP.

The results (Fig. 2) revealed in contrast to our prediction from the COMPARE analyses that while **7a** did not show noteworthy kinase inhibition **5c** inhibited seven receptor tyrosine kinases (EGFR, Erb-b2, IGF1-R, VEGFR-R1,

Table 2. Results of a matrix COMPARE analysis^a of the series **5** and **7**

Compound	7h^b	7g	7f	7e	7d	7c	7b	7a	5g	5f	5e	5d	5c	5b
5a	0.144 (54)	-0.021 (54)	0.164 (54)	0.006 (54)	0.176 (54)	0.168 (54)	-0.067 (54)	0.222 (44)	0.226 (45)	0.4 (54)	0.199 (54)	0.22 (54)	0.436 (54)	0.356 (54)
5b	0.069 (55)	0.377 (54)	0.228 (55)	0.101 (55)	0.196 (55)	0.115 (55)	0.024 (55)	0.221 (44)	0.069 (55)	0.604 (55)	0.228 (55)	0.406 (55)	0.444 (55)	
5c	0.037 (56)	0.246 (55)	-0.146 (56)	-0.167 (56)	0.036 (56)	-0.2 (56)	-0.149 (56)	-0.018 (45)	0.331 (47)	0.757 (56)	0.482 (56)	0.615 (56)		
5d^b	-0.112 (60)	0.065 (59)	-0.125 (60)	-0.191 (60)	0.008 (60)	-0.016 (60)	-0.035 (60)	-0.092 (49)	0.429 (50)	0.64 (56)	0.675 (60)			
5e^b	0.007 (60)	0.297 (59)	0.008 (60)	-0.146 (60)	0.109 (60)	0.026 (60)	0.055 (60)	0.16 (49)	0.267 (50)	0.524 (56)				
5f	0.074 (56)	0.331 (55)	0.029 (56)	-0.059 (56)	0.139 (56)	-0.012 (56)	-0.065 (56)	0.071 (45)	0.199 (47)					
5g	-0.074 (50)	-0.054 (49)	-0.171 (50)	-0.08 (50)	-0.169 (50)	-0.036 (50)	-0.278 (50)	0.069 (40)						
7a	0.611 (49)	0.44 (49)	0.585 (49)	0.607 (49)	0.599 (49)	0.569 (49)	0.64 (49)							
7b^b	0.487 (60)	0.457 (59)	0.469 (60)	0.556 (60)	0.693 (60)	0.647 (60)								
7c^b	0.623 (60)	0.396 (59)	0.786 (60)	0.523 (60)	0.72 (60)									
7d^b	0.821 (60)	0.683 (59)	0.647 (60)	0.653 (60)										
7e^b	0.677 (60)	0.426 (59)	0.649 (60)											
7f^b	0.705 (60)	0.55 (59)												
7g^b	0.591 (59)													

^a The correlation (Pearson correlation coefficient) between the distinct compounds as calculated from a matrix COMPARE analysis is given. Numbers in brackets correspond to the number of cell lines that were used for calculation. The data given in bold italics are considered significant ($p < 0.01$). The distinct p values were calculated from the PCCs and the number of cell lines by StatTable vers.1.0.2 (Cytel Software, Cambridge, MA 02139, USA).

^b Average of 2 experiments.

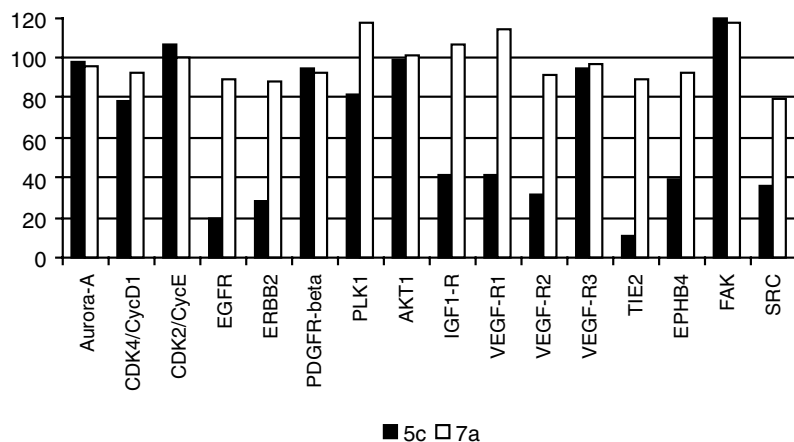


Figure 2. Residual activities [%] of cancer-related protein kinases after incubation with 10 μ M diaryl-3-hydroxy-2,3,3a,10a-tetrahydrobenzo[b]cyclopenta[e]azepine-4,10(1H,5H)-diones **5c** (■) or **7a** (□); ATP concentration, 0.1 μ M. The displayed diagram represents one of two tests runs which were performed in singlicate, respectively. In the second run, 1 μ M test compound was used (data not shown). As parameter of the assay quality, the Z' factor¹⁷ was calculated, which did not drop below 0.43 and exceeded 0.70 in most cases. As an additional control, for the distinct enzymes the coefficients of variation (CV) of a 1% DMSO plate ($n = 88$) were calculated, which did not exceed 13.39% and were lower than 10% in most cases.

VEGF-R2, TIE2, and EPHB4) by more than 50%. Based on these findings we speculate that the modest antiproliferative activity of compounds **5** might be caused by a moderate unselective inhibition of receptor tyrosine kinases. It is surprising that although most of the compounds **7** showed a positive correlation with the EGF-receptor expression (MT1093, Table 1) neither this nor any other of the tested receptor kinases was inhibited by **7a**. Besides a direct kinase inhibition by **7a**, which seems unlikely based on our findings, several other putative mechanisms can be used as hypotheses for an explanation of the observed correlation with the molecular targets of Table 1. For instance, compounds **7** could interact with molecules of signaling cascades in which the kinases are involved. Furthermore, it should be considered that the molecular targets in the IVCLSP might be intercorrelated with other cancer-relevant molecules that have not yet been screened and constitute the actual biological target. For instance, the expression of the two mentioned tyrosine kinases in the IVCLSP is highly intercorrelated with a PCC of 0.776.

In conclusion, we have disclosed diastereoselective syntheses¹⁸ of two closely related antiproliferative compound series **5** and **7** which are clearly distinguished by the bioinformatic tool COMPARE. Although protein kinases apparently are involved in the growth inhibitory activity displayed by **5** and **7**, a defined mechanism still has to be established. Based on the preliminary results reported here, further investigations addressing the antiproliferative mechanism as well as the role of single enantiomers of the title compounds appear promising.

Acknowledgments

We thank the National Cancer Institute for testing of the compounds in the In Vitro Cell Line Screening Project. Funding by the Deutsche Forschungsgemeinschaft (Ku 1371/1, to C.K. and C.P.) and the European Commission (Contract No LSHB-CT-2004-503467, to

C.K., F.T., C.S., and M.H.G.K.) is gratefully acknowledged.

References and notes

- Link, A.; Kunick, C. *J. Med. Chem.* **1998**, *41*, 1299.
- Link, A.; Zaharevitz, D. W.; Kunick, C. *Pharmazie* **1999**, *54*, 163.
- Schultz, C.; Link, A.; Kunick, C. *Arch. Pharm. Med. Chem.* **2001**, *334*, 163.
- Kunick, C. *Curr. Med. Chem. Anti-Cancer Agents* **2004**, *4*, 421.
- Fiesselmann, H.; Ribka, J. *Chem. Ber.* **1956**, *89*, 40.
- Ball, H.; Schneider, M. R.; Schoenenberger, H. *Arch. Pharm. (Weinheim, Germany)* **1984**, *317*, 565.
- Schönenberger, H.; Bastug, T.; Adam, D. *Arzneim.-Forsch.* **1969**, *19*, 1082.
- Kotera, K.; Takano, Y.; Matsuura, A.; Kitahonoki, K. *Tetrahedron* **1970**, *26*, 539.
- Boyd, M. R.; Paull, K. D. *Drug Dev. Res.* **1995**, *34*, 91.
- Monks, A.; Scudiero, D.; Skehan, P.; Shoemaker, R.; Paull, K.; Vistica, D.; Hose, C.; Langley, J.; Cronise, P.; Vaigro-Wolff, A.; Gray-Goodrich, M.; Campbell, H.; Mayo, J.; Boyd, M. *J. Natl. Cancer Inst.* **1991**, *83*, 757.
- Paull, K. D.; Shoemaker, R. H.; Hodes, L.; Monks, A.; Scudiero, D. A.; Rubinstein, L.; Plowman, J.; Boyd, M. R. *J. Natl. Cancer Inst.* **1989**, *81*, 1088.
- Monks, A.; Scudiero, D. A.; Johnson, G. S.; Paull, K. D.; Sausville, E. A. *Anti-Cancer Drug Des.* **1997**, *12*, 533.
- Weinstein, J. N.; Myers, T. G.; O'Connor, P. M.; Friend, S. H.; Fornace, A. J., Jr.; Kohn, K. W.; Fojo, T.; Bates, S. E.; Rubinstein, L. V.; Anderson, N. L.; Buolamwini, J. K.; van Osdol, W. W.; Monks, A. P.; Scudiero, D. A.; Sausville, E. A.; Zaharevitz, D. W.; Bunow, B.; Viswanadhan, V. N.; Johnson, G. S.; Wittes, R. E.; Paull, K. D. *Science* **1997**, *275*, 343.
- Sun, W.; Fujimoto, J.; Tamaya, T. *Oncology* **2004**, *66*, 450.
- Normanno, N.; Bianco, C.; Strizzi, L.; Mancino, M.; Maiello, M.; De Luca, A.; Caponigro, F.; Salomon, D. *Curr. Drug Targets* **2005**, *6*, 243.
- Medinger, M.; Drevs, J. *Curr. Pharm. Des.* **2005**, *11*, 1139.

17. Zhang, J.; Chung, T.; Oldenburg, K. *J. Biomol. Screen.* **1999**, *4*, 67.
18. Synthesis of **7a**, typical procedure: to a stirred suspension of **3** (175 mg, 1.0 mmol) in ethanol (4 mL) is added potassium hydroxide (112 mg, 2.0 mmol). After stirring of the mixture for 5 min at room temperature, **6a** (290 mg, 1.0 mmol) is added and stirring is continued for 6 h. The pH is adjusted to 6 by addition of acetic acid. The precipitate is collected and crystallized from ethanol to yield **7a** (170 mg, 44%) as colorless crystals, IR: 3440 (OH), 3185 (NH), 3050 (C-H arom.), 1650 (C=O) cm^{-1} ; ^1H NMR: (400 MHz, d_6 -DMSO) δ (ppm) = 2.59 (dd, 1H, $J = 12.7/12.7$ Hz, H₁), 2.85 (ddd, 1H, $J = 12.1/8.6/3.0$ Hz, H-1) 3.29–3.36 (m, 1H, H-2), 3.68 (dt, 1H, $J = 11.2/11.2/3.0$ Hz, H-10a), 3.80 (d, 1H, $J = 12.2$ Hz, H-3a), 5.43 (d, 1H, $J = 1.6$ Hz, OH), 7.03–7.13 (m, 6H, H arom.), 7.16 (t, 2H, $J = 7.2/7.2$ Hz, H arom.), 7.21 (d, 1H, $J = 7.6$ Hz, H arom.), 7.28 (t, 1H, $J = 7.6/7.6$ Hz, H arom.), 7.38 (d, 2H, $J = 7.1$ Hz, H arom.), 7.59 (ddd, 1H, $J = 7.6/7.6/1.5$ Hz, H arom.), 8.16 (dd, 1H, $J = 8.1/1.5$ Hz, H arom.), 10.47 (s, 1H, NH); ^1H - ^1H COSY: (400 MHz, d_6 -DMSO) selected cross signals: 2.59 and 2.85 with 3.33, 3.33 with 5.43, 3.68 with 2.59 and 2.85 and 3.80; NOESY: (500 MHz, d_6 -DMSO) see legend of Figure 1; ^{13}C NMR: (100.62 MHz, d_6 -DMSO) δ (ppm) = 30.6 (CH₂), 49.5, 51.2, 55.4 (C tert.), 83.4 (C-OH), 122.1, 123.7, 125.4, 126.2, 127.2, 127.4, 129.2, 130.6, 134.1 (C tert.), 124.8, 137.7, 138.2, 143.4 (C quat.), 174.3 (lactam C=O), 196.6 (C=O); C₂₅H₂₁NO₃ (383.45) calcd C 78.31; H 5.52, N 3.65; found C 78.33, H 5.59, N 3.69.